Procedia Computer Science

Volume 80, 2016, Pages 1354–1363

ICCS 2016. The International Conference on Computational Science

Multi-Scale Coupling Between Monte Carlo Molecular Simulation and Darcy-Scale Flow in Porous Media

Ahmed Saad, Ahmad Kadoura, and Shuyu Sun*

King Abdullah University of Science and Technology (KAUST), Physical Science and Engineering Division (PSE), Computational Transport Phenomena Laboratory (CTPL), Thuwal 23955-6900, Saudi Arabia.

ahmed.mohamedsaad@kaust.edu.sa

ahmad.kadoura@kaust.edu.sa

shuyu.sun@kaust.edu.sa

Abstract

In this work, an efficient coupling between Monte Carlo (MC) molecular simulation and Darcy-scale flow in porous media is presented. The cell centered finite difference method with non-uniform rectangular mesh were used to discretize the simulation domain and solve the governing equations. To speed up the MC simulations, we implemented a recently developed scheme that quickly generates MC Markov chains out of pre-computed ones, based on the reweighting and reconstruction algorithm. This method astonishingly reduces the required computational times by MC simulations from hours to seconds. To demonstrate the strength of the proposed coupling in terms of computational time efficiency and numerical accuracy in fluid properties, various numerical experiments covering different compressible single-phase flow scenarios were conducted. The novelty in the introduced scheme is in allowing an efficient coupling of the molecular scale and the Darcy's one in reservoir simulators. This leads to an accurate description of thermodynamic behavior of the simulated reservoir fluids; consequently enhancing the confidence in the flow predictions in porous media.

Keywords: Monte Carlo molecular simulation, Reservoir modelling, Darcy flow, Reweighting and reconstruction, NVT and NpT ensembles

1 Introduction

It is crucial for reservoir flow simulators to have efficient thermodynamic models that accurately describe the phase behaviour of the subsurface fluids. So far, continuum-based models (e.g. equations of state and correlations) have played the major role in fulfilling the task [1, 2]. Nonetheless, with the increase in exploiting the non-conventional reservoirs, the continuum-based models have faced two main challenges [3, 4]: (i) Lack of experimental data availability

*Corresponding author. Tel.: +966-544-700-084. E-mail address: shuyu.sun@kaust.edu.sa

 Selection and peer-review under responsibility of the Scientific Programme Committee of ICCS 2016

doi:10.1016/j.procs.2016.05.428

due to operating under extreme pressure and/or temperature conditions, in addition to presence of hazardous materials (e.g. corrosive, toxic and explosive). (ii) Working at extremely small scale (e.g. tight formations and shale gas reservoirs).

On the other hand, Monte Carlo (MC) molecular simulation, which is based on statistical thermodynamics principles [5–8], is capable of overcoming these challenges; however it imposes a high computational cost. This computational burden has made it infeasible to replace correlations by MC molecular simulations in order to describe fluid thermodynamic properties in flow simulators. Recently, we have proposed several techniques aiming to overcome this obstacle. In doing that, two strategies have been adapted. The first strategy tries to accelerate MC simulations by modifying the original algorithm itself [9] via proposing the conservative [10] and the non-conservative [11] early rejection algorithms. The second strategy works by extracting more information from the pre-generated MC Markov chains, such that a single simulation can be used to replace multiple ones. For this purpose, the reweighting and reconstruction method [12, 13] has been developed in addition to the NVT-NpT switching scheme [14].

In this article, a novel multi-scale coupling between Darcy-scale flow and MC molecular simulation is presented. In all the investigated cases a compressible single-phase methane reservoir is simulated under various isothermal production and geophysical scenarios. In distinctive manner from the classical approach, few pre-computed MC Markov chains were only used to feed the flow simulator with the necessary thermodynamic properties at wide range of pressures. It is worth to mention that these thermodynamic properties (fluid density and isothermal compressibility) are needed by the simulator at every discretized cell at every time step. For this particular reason, it is infeasible to run a full independent MC molecular simulation, which may need more than 30 minutes for each cell at every time step using an Intel 2.67 GHz processor. For instance, in this work an order of hundreds of discretized cells was used. Fortunately, the reweighting and reconstruction method enables us to use and reuse few pre-computed MC Markov chains to accurately predict fluid properties at neighboring thermodynamic conditions within fraction of a second.

In the following sections of the paper, a brief description about the reweighting and reconstruction method and its switching scheme is provided. Moreover, a complete set of flow governing equations are listed and discussed. Finally, the flow simulation results for different methane reservoirs are presented.

2 Simulation Methods

2.1 Flow governing equations

The cell centered finite difference method for compressible single-phase single-component system was used. The system was reduced to a set of linear equations in which the pressure field was the primary unknown. Then using MATLAB's linear solver, these equations were implicitly solved employing a constant time step. Simulations with uniform and non-uniform rectangular mesh were both considered. The governing equations that describe the system are:

The mass conservation law:

The mass conservation law equates the difference between the input and the output fluxes

to the accumulation term in the unit cell:

$$\frac{\partial(\phi\rho)}{\partial t} + \nabla.(\rho\mathbf{u}) = q. \tag{1}$$

In Equation 1, ϕ is the rock porosity, ρ is the mass density, $\mathbf{u}$ is the darcy velocity , q is the mass source and t is the time. Based on the definition of the isothermal compressibility, the mass conservation law can be formulated in terms of pressure instead of density as follows:

$$\phi\rho C_T \frac{\partial p}{\partial t} + \nabla.(\rho\mathbf{u}) = q, \tag{2}$$

where p is the pressure and C_T is the isothermal compressibility.

Darcy velocity equation:

$$\mathbf{u} = -\frac{k}{\mu}\nabla p. \tag{3}$$

Under the assumption of no gravitational field effect, the Darcy's law takes the form in Equation 3; where, k and μ are the rock permeability and fluid viscosity, respectively.

Production well model:

In describing flow around wells, the well known Peaceman radial well model [15] was employed:

$$q = WI\,(p_{bh} - p_c)\,, \tag{4}$$

$$WI = \frac{2\pi\rho\sqrt{k_x k_y}h_z}{\mu ln(\frac{r_e}{r_w})}. \tag{5}$$

In the Peaceman model, WI is the well index, k_x and k_y are the permeabilities in the x and y directions respectively, h_z is the vertical thickness, p_{bh} is the well bottom hole pressure, p_c is the cell average pressure, r_e is the cell equivalent radius and r_w is the well radius.

2.2 Reservoir fluid properties

Viscosity:

The natural gas correlation by Lee et al. [16] was adopted in order to compute methane viscosity as function of pressure and temperature:

$$\mu_g = K_1 e^{X\rho^Y}, \tag{6}$$

$$K_1 = \frac{(0.00094 + 2\times10^{-6}M)^{1.5}}{(209 + 19M + T)}, \tag{7}$$

$$X = 3.5 + \frac{986}{T} + 0.01M,\ Y = 2.4 - 0.2X. \tag{8}$$

In the equations above, μ_g is the viscosity in cp, ρ is the density in g/cm^3, p is the pressure in psia, T is the temperature in R and M is the gas molecular weight.

Density:

The fluid density was estimated using the pre-computed MC molecular simulation results, solving the non-linear inverse problem for the known pressure using the NVT-NpT switching scheme [14]. For each Markov chain an MC simulation of 216 LJ particles were simulated in NVT ensemble for 10×10^6 and 20×10^6 steps corresponding to equilibrium and production, respectively.

In MC molecular simulation, macroscopic properties are usually obtained by averaging configurational quantities. Tail corrections are preferentially considered to account for the domain truncation errors. The first direct macroscopic output of the NVT ensemble is often pressure. The system's normalized pressure p^* can be evaluated using the equations below:

$$p^* = \frac{p\sigma^3}{\varepsilon} = \frac{\rho^*}{\beta^*} + \frac{\rho^*}{N}\left\langle V^* \right\rangle_{can} + p^*_{tail}, \tag{9}$$

$$\left\langle V^* \right\rangle_{can} = \frac{\sum_{k=1}^{M} \exp\left(-w_k\right) V_k^*}{\sum_{k=1}^{M} \exp\left(-w_k\right)} \tag{10}$$

$$V_k^* = \frac{V_k}{\varepsilon} = 8 \sum_{i<j} \left[2\left(\frac{1}{L^* s_{ij}^*}\right)^{12} - \left(\frac{1}{L^* s_{ij}^*}\right)^{6} \right], \tag{11}$$

$$p^*_{tail} = \frac{16}{3}\pi\rho^{*2}\left[\frac{2}{3}\left(\frac{1}{L^* s_c^*}\right)^{9} - \left(\frac{1}{L^* s_c^*}\right)^{3}\right];\ s_c = \frac{r_c^*}{L^*} = 0.49, \tag{12}$$

Equation 11 represents a pre-defined configurational property that is solely dependent on the particles distances distribution in the simulated system. The model parameters ε and σ are related to the nature of the simulated particle, N is the total number of particles, β^* is the normalized Boltzmann's factor and equivalent to the reciprocal of the normalized temperature ($T^* = T/(\varepsilon/k_B)$), k_B is the Boltzmann's constant and ρ^* is the normalized number density ($\rho^* = \rho\sigma^3$). Moreover, L^* and s_{ij}^* are the normalized simulation box length ($L^* = L/\sigma$) and the normalized distances between any pair of particles i and j ($s_{ij}^* = r_{ij}^*/L^*$), respectively. Whereas, $\langle V^* \rangle_{can}$ stands for the canonical average of V^* over all the sampled configurations, which is normally evaluated using Equation 10 with all the weights w_k set to zero to obtain the arithmetic average of the configurations. The pressure tail correction function p^*_{tail} is used to count for truncated interactions beyond the imposed cutoff radius r_c^*.

Implementing the setup above, one can successfully evaluate p^* for any given MC Markov chain at a certain ρ^* and β^*. Furthermore, the forward reweighting and reconstruction scheme makes it possible to use a single Markov chain at a certain ρ^* and β^* to predict pressures at neighboring thermodynamic conditions ($\rho^*+\Delta\rho^*$, $\beta^*+\Delta\beta^*$). Along Isotherms, the source Markov chain to be used for extrapolation is first reconstructed by rescaling interactions with

the new box length corresponding to the new density ($\rho^*+\Delta\rho^*$). After rescaling, the reconstructed Markov chain is reweighted with the following weighting factor (w_k):

$$w_k = \beta_o^* \left[U_k^* \left(\beta_o^*, L_n^*\right) - U_k^* \left(\beta_o^*, L_o^*\right)\right] + N\beta_o^* \left[E_{tail}^* \left(L_n^*\right) - E_{tail}^* \left(L_o^*\right)\right], \tag{13}$$

$$U_k^* = \frac{U_k}{\varepsilon} = 4\sum_{i<j}\left[\left(\frac{1}{L^* s_{ij}^*}\right)^{12} - \left(\frac{1}{L^* s_{ij}^*}\right)^{6}\right], \tag{14}$$

$$E_{tail}^* = \frac{8}{3}\pi\rho^*\left[\frac{1}{3}\left(\frac{1}{L^* s_c^*}\right)^{9} - \left(\frac{1}{L^* s_c^*}\right)^{3}\right]. \tag{15}$$

It is important to highlight that the above formulation is solving an NVT problem starting from an MC Markov chain generated by an NVT ensemble simulation. However, within the flow simulator environment, an NpT problem exists. For this particular reason, switching scheme was originally developed [14].

Isothermal compressibility:

Once the unknown fluid densities corresponding to the given pressures at each cell were evaluated, the fluid isothermal compressibility was estimated via the forward reweighting and reconstruction method. The inverse of the normalized isothermal compressibility (C_T^{*-1}) was evaluated using the following formula [14]:

$${C_T}^{*-1} = \frac{{C_T}^{-1}\sigma^3}{\varepsilon} = \frac{\rho^*}{\beta^*} + \rho^*\left\langle W^*\right\rangle_{can} - 2\beta^*\rho^{*2}\left(\left\langle V^{*2}\right\rangle_{can} - \left\langle V^*\right\rangle_{can}^2\right) + C_{tail}^*\,, \tag{16}$$

$$W_k^* = \frac{W_k}{\varepsilon} = 8\sum_{i<j}\left[10\left(\frac{1}{L^* s_{ij}^*}\right)^{12} - 3\left(\frac{1}{L^* s_{ij}^*}\right)^{6}\right]. \tag{17}$$

In the equations above, W_k^* stands for an additional configurational quantity that is dependent on the distances among all the existing LJ particles in the simulation. C_{tail}^* corresponds to the correction function used to count for truncated interactions beyond the imposed cutoff radius ($r_c^* = 0.49L^*$). For more details in how forward reweighting and reconstruction is performed, the reader is referred to [13]. Figure 1 summarizes the work flow of combining the forward reweighting and reconstruction with the switching scheme. First, the inverse problem discussed earlier is solved to evaluate the fluid densities out of a given pressure (Figure 1.a). After the pressure is known, the isothermal compressibility can be directly evaluated via the forward reweighting and reconstruction method (Figure 1.b).

3 Results and Discussion

The proposed coupling was tested with various production scenarios from methane gas reservoirs (Methane LJ parameters are: ϵ/k_B= 147.4 K and σ = 3.722 Å) at isothermal condition (T

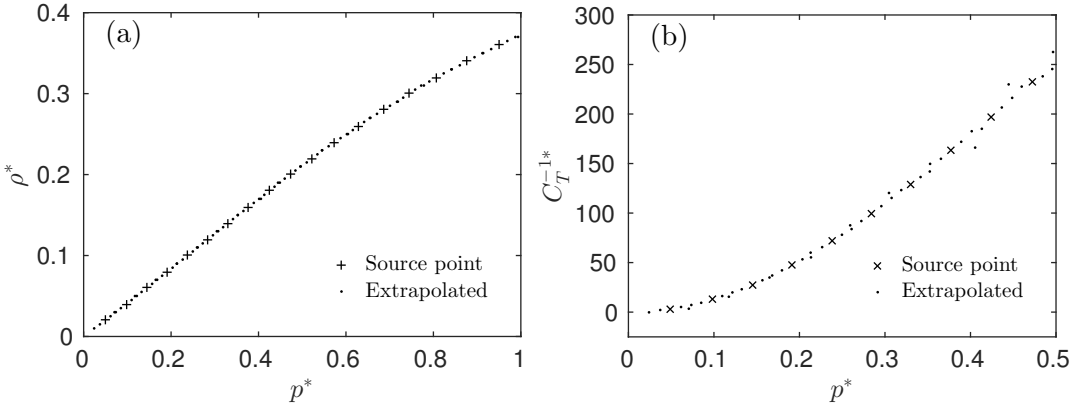

Figure 1: (a) Normalized number density (ρ^*) versus normalized pressure (p^*) along β^*=0.4 (T=368.5 K) isotherm. (b) Inverse of normalized isothermal compressibility C_T^{*-1} versus normalized pressure p^* along β^*=0.4. Source points of extrapolation are plotted as crosses while extrapolated points are plotted as dots. Two points are extrapolated out of each source point in both directions.

= 368.5 K). These reservoirs have different configurations with a 2D domain covering 240 m × 240 m area of 0.2 porosity with Neumann no flow boundary condition. In all the studied scenarios, the production lasted for 200 days, while the initial reservoir pressure and the well down-hole pressure were 200 and 100 atm, respectively. The proposed multi-scale coupling algorithm between MC molecular simulation and Darcy flow, used in simulating the studied cases in this paper, is given in Figure 2.

3.1 Homogeneous reservoir test case

In the first scenario, a homogeneous permeability field of 100 md was imposed throughout the reservoir domain which was discretized as 80 × 80 cells. A single production well was placed at the center. Figure 3 shows the contour plot of pressure field with the velocity streamlines and the production rate profile relative to initial production. As expected, the pressure and velocity fields are symmetric around the wellbore because of the homogeneity of the domain properties.

3.2 Heterogeneous reservoir test case

In the second scenario, a heterogeneous permeability field with values ranging from less than 1 md to about 200 md was imposed throughout the reservoir domain with a single production well at the center with 50 × 50 cells discretized domain. The effect of the heterogeneous medium is clearly seen in the irregular shape of the streamlines and the pressure contour plot (Figure 4.b). In this case the production rate decline is slower than the homogeneous case (Figures 3.a and 4.a) although the overall average rock permeability in the two cases is almost the same. This is mainly because of the presence of dead zones in the heterogeneous reservoir that have very low permeability and as a result, the reservoir is depleted at slower rates.

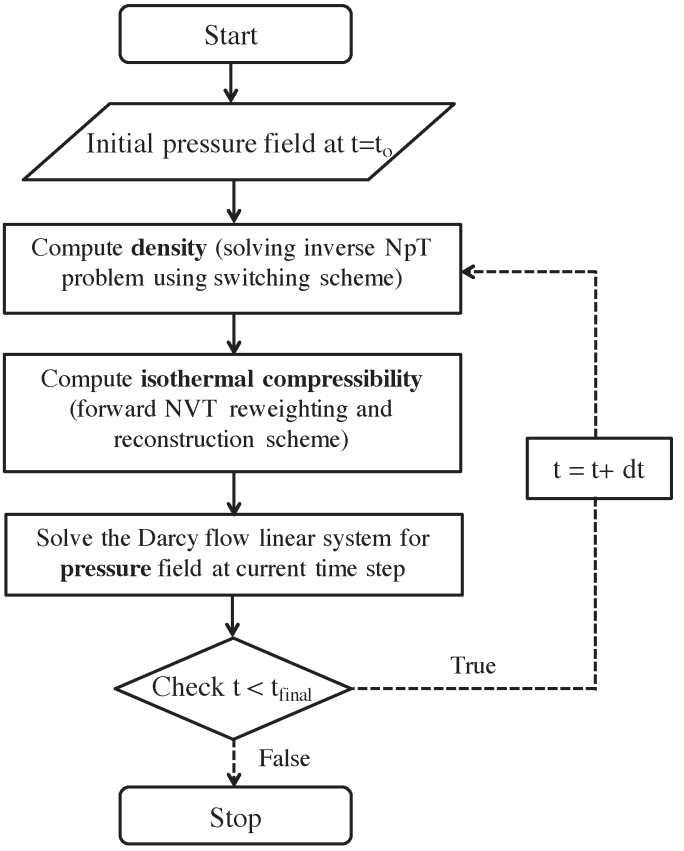

Figure 2: MC simulation and Darcy scale coupling algorithm.

3.3 Fractured reservoir test case 1

A fractured reservoir case was also investigated, where a homogeneous matrix permeability of 100 md throughout the domain was imposed with four crossing fractures of 3 cm width with permeability of 1000 d. The well was placed at the center passing through the matrix. The domain was discretized as 80 × 80 cells so that each had a dimension of 3 m × 3m. Originally, a dramatic drop of the flow rate is observed (Figure 5.a) as the center reservoir block is depleted. Later, the production rate resumes in similar fashion compared to the previous scenarios as the fractures communicate the pressure disturbance to the neighboring blocks. Due to the symmetricity in placing the fractures relative to the production well, the streamlines and pressure field are symmetric too (Figure 5.b).

3.4 Fractured reservoir test case 2

The only difference in the reservoir setup in this case from the third one is the well location. Here the production well was located at the intersection of the two fractures, instead of being placed at the matrix. The effect of the new well location is evident in Figure 6. In addition, it can be clearly seen that the overall production rate decline is much sharper in this scenario than in the third one because of the well intersection with the two fractures.

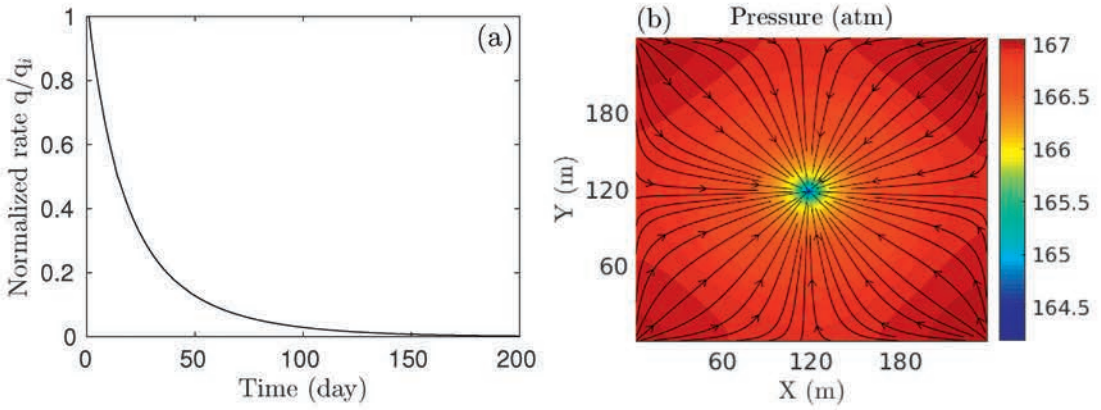

Figure 3: Homogeneous reservoir case: (a) Normalized production rate profile. (b) Pressure contour map with darcy velocity streamlines after 10 days of production.

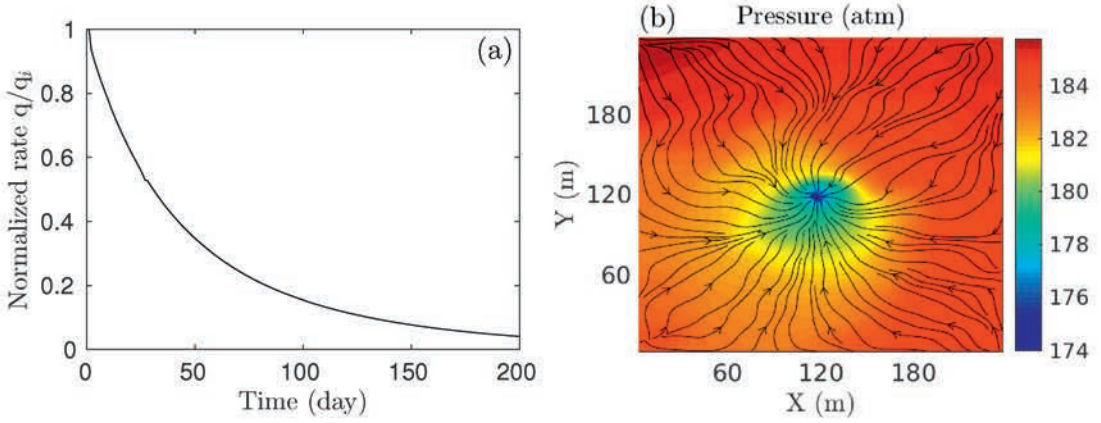

Figure 4: Heterogeneous reservoir case: (a) Normalized production rate profile. (b) Pressure contour map with darcy velocity streamlines after 10 days of production.

4 Conclusion

An efficient coupling between MC molecular simulation and Darcy flow simulation in porous media was developed using the reweighting and reconstruction method along with NVT-NpT switching scheme. The proposed combination was tested on methane system in different reservoir configurations. The accurate description of thermodynamic behavior of the simulated reservoir fluids using MC Molecular simulation decreases the uncertainty in reservoir simulation predictions. The reweighting and reconstruction technique allows extrapolation in seconds instead of running the typical molecular simulation for hours. In conclusion, the implementation of the reweighting and reconstruction method using few offline, pre-computed Markov chains has made it computationally feasible to benefit from the molecular simulation accuracy in determining phase properties needed by the reservoir simulator. For the future work, we will consider more realistic flow scenarios in subsurface reservoirs. In addition, An interesting work is using different potential models in addition to the LJ model to be able to simulate other

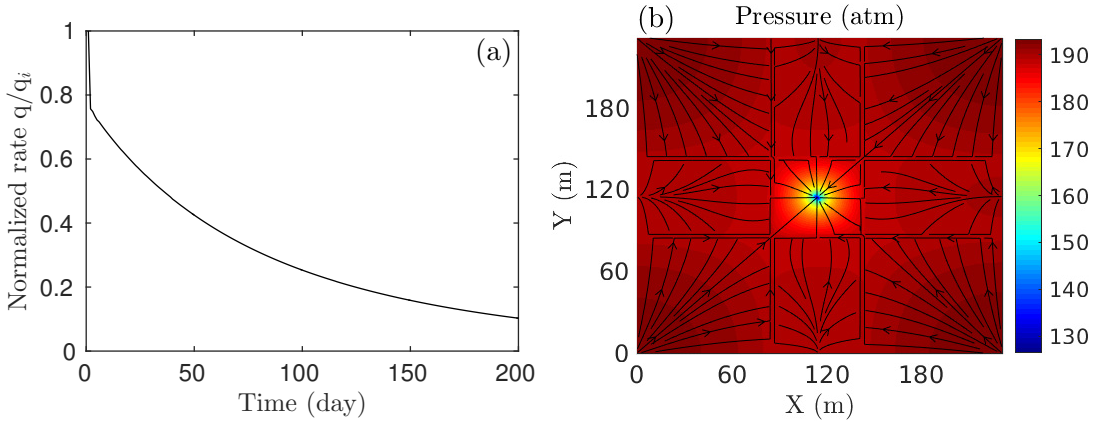

Figure 5: Fractured reservoir case 1: (a) Normalized production rate profile. (b) Pressure contour map with darcy velocity streamlines after 10 days of production.

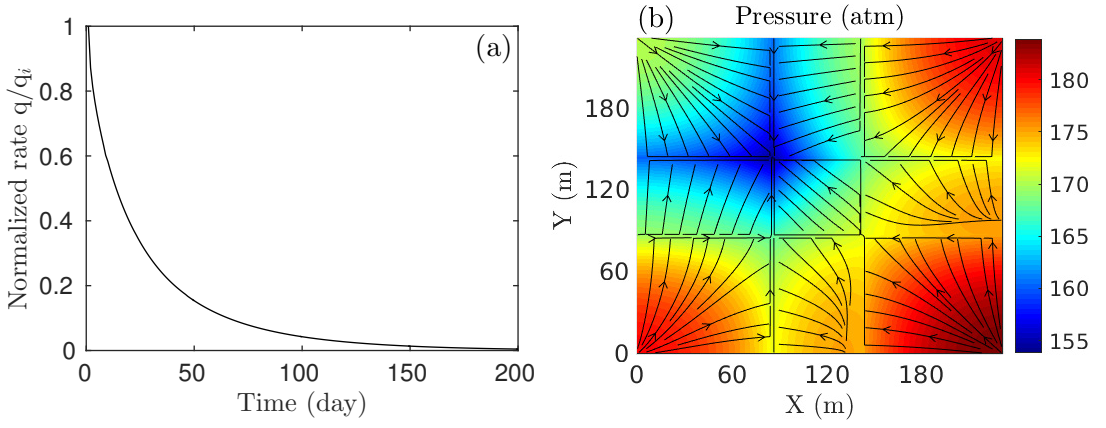

Figure 6: Fractured reservoir case 2: (a) Normalized production rate profile. (b) Pressure contour map with darcy velocity streamlines after 10 days of production.

fluids with quadrupole moment such as CO_2 and extending the reweighting and reconstruction method to work with other ensembles to simulate multi-phase systems.

Acknowledgments

The research reported in this publication was supported by funding from King Abdullah University of Science and Technology (KAUST).

References

[1] Abbas Firoozabadi. *Thermodynamics of Hydrocarbon Reservoirs.* McGraw Hill Professional, USA, 1999.

[2] Abbas Firoozabadi. *Thermodynamics and Applications of Hydrocarbons Energy Production*. McGraw Hill Professional, USA, 2015.

[3] P. Ungerer, V. Lachet, and B. Tavitian. Applications of molecular simulation in oil and gas production and processing. *Oil Gas Sci. Technol.*, 61:387–403, 2006.

[4] P. Ungerer, C. Nieto-Draghi, V. Lachet, A. Wender, A. di Lella, A. Boutin, B. Rousseau, and A. H. Fuchs. Molecular simulation applied to fluid properties in the oil and gas industry. *Mol. Simulat.*, 33(4–5):287–304, 2007.

[5] M. P. Allen and D. J. Tildesley. *Computer Simulation of Liquids*. Oxford University Press, USA, 1989.

[6] R. L. Rowley. *Statistical Mechanics for Thermophysical Property Calculations*. Prentice Hall, USA, 1994.

[7] D. A. McQuarrie. *Statistical Mechanics*. University Science Books, California, USA, 2000.

[8] Daan Frenkel and Berend Smit. *Understanding Molecular Simulation: From Algorithms to Applications*. Academic Press, San Diego, CA, 2001.

[9] N. Metropolis, A. W. Rosenbluth, M. N. Rosenbluth, A. H. Teller and E. Teller. Equation of state calculations by fast computing machines. *J. Chem. Phys.*, 21:1087–1092, 1953.

[10] A. Kadoura, A. Salama, and S. Sun. A conservative and a hybrid early rejection schemes for accelerating Monte Carlo molecular simulation. *Mol. Phys.*, 112(19):2575–2586, 2014.

[11] A. Kadoura, A. Salama, and S. Sun. Speeding up Monte Carlo molecular simulation by a non-conservative early rejection scheme. *Mol. Simulat.*, 42(3):241–241, 2015.

[12] S. Sun, A. Kadoura, and A. Salama. An efficient method of reweighting and reconstructing monte carlo molecular simulation data for extrapolation to different temperature and density conditions. In *13th International Conference on Computational Science*, Procedia Computer Science, pages 2147–2156. Elsevier, 5–7 June 2013.

[13] A. Kadoura, S. Sun, and A. Salama. Accelerating Monte Carlo molecular simulations by reweighting and reconstructing Markov chains: Extrapolation of canonical ensemble averages and second derivatives to different temperature and density conditions. *J. Comput. Phys.*, 270(4):70–85, 2014.

[14] A. Kadoura, A. Salama, and S. Sun. Switching between the NVT and NpT ensembles using the reweighting and reconstruction scheme. In *15th International Conference on Computational Science*, Procedia Computer Science, pages 1259–1268. Elsevier, 1–3 June 2015.

[15] D. W. Peaceman. Interpretation of Well-Block Pressures in Numerical Reservoir Simulation. *SPE Journal*, 18(03):183–194, 1978.

[16] A. L. Lee, M. H. Gonzalez, and B. E. Eakin. The Viscosity of Natural Gases. *JPT*, 18(08):997–1000, 1966.